nature structural & molecular biology

Cryo-EM structure of the ribosome–SecYE complex in the membrane environment

Jens Frauenfeld[1,2], James Gumbart[3], Eli O van der Sluis[1,2], Soledad Funes[4], Marco Gartmann[1,2], Birgitta Beatrix[1,2], Thorsten Mielke[5], Otto Berninghausen[1,2], Thomas Becker[1,2], Klaus Schulten[3] & Roland Beckmann[1,2]

The ubiquitous SecY–Sec61 complex translocates nascent secretory proteins across cellular membranes and integrates membrane proteins into lipid bilayers. Several structures of mostly detergent-solubilized Sec complexes have been reported. Here we present a single-particle cryo-EM structure of the SecYEG complex in a membrane environment, bound to a translating ribosome, at subnanometer resolution. Using the SecYEG complex reconstituted in a so-called Nanodisc, we could trace the nascent polypeptide chain from the peptidyltransferase center into the membrane. The reconstruction allowed for the identification of ribosome–lipid interactions. The rRNA helix 59 (H59) directly contacts the lipid surface and appears to modulate the membrane in immediate vicinity to the proposed lateral gate of the protein-conducting channel (PCC). On the basis of our map and molecular dynamics simulations, we present a model of a signal anchor–gated PCC in the membrane.

The vast majority of proteins designated to be secreted or to be integrated into the membrane bilayer have to pass the ubiquitous PCC, termed the Sec61 complex in eukaryotes or SecYEG in prokaryotes[1]. In the co-translational mode, when the hydrophobic signal sequence or signal anchor of a nascent polypeptide chain emerges from the ribosome, the ribosome–nascent chain complex (RNC) is targeted to the membrane by the signal-recognition particle (SRP) and the SRP receptor[2]. After transfer from the SRP system to the PCC, the ribosome continues translation while the nascent polypeptide is directly guided from the ribosomal exit tunnel into the ribosome-bound SecY–Sec61 complex for membrane translocation or integration.

The PCC is conserved among all organisms, and several crystal structures of detergent-solubilized PCCs have been reported[3–6], sharing a common core of 12 transmembrane (TM) helices. This core consists of one large and two small subunits, termed SecY–Sec61α, SecE–Sec61γ and SecG–Sec61β, respectively (the latter is less conserved). In *Escherichia coli*, SecY is composed of two pseudosymmetric halves comprising the N-terminal TM1–TM5 and C-terminal TM6–TM10 helices. SecY is flanked by the clamp-like protein SecE, composed of three TM helices and an amphipathic helix, and SecG, which consists of two TM helices. The PCC may open both perpendicular to the plane of the membrane for the translocation of soluble polypeptides across the membrane, and laterally for the integration of TM helices into the membrane. To that end, the two clamshell-like halves of SecY have been suggested to open on one side in order to form a lateral gate that can accommodate the signal sequence or the signal anchor[4–7]. Consistent with this idea, three recent crystal structures of SecYE show a partial opening of the lateral gate[4–6]. After the gating event, the polypeptide is thought to use the central hourglass-shaped aqueous vestibule of the Sec complex as a conduit for translocation[8]. The central plug helix 2a of SecY would move, and the central hydrophobic pore ring would provide a flexible seal to avoid ion leakage across the membrane[1]. Although a low-resolution cryo-EM structure of a programmed ribosome–SecYEG complex was interpreted as comprising two copies of the SecYEG complex forming a joint pore[9], more recent biochemical, structural and simulation data show that a single copy of the Sec complex is most likely forming the active PCC[10–14]. All three-dimensional (3D) structures of the PCC bound to the ribosome, however, were obtained using detergent-solubilized Sec complexes[6,9–11,13,15–19]. It has been shown that, in principle, the PCC can be active in detergent solution[20]; however, it is not clear to what extent the absence of the lipid bilayer may influence the structure and activity of the PCC. Thus, the conformation of the ribosome–Sec complex in its natural environment remains to be elucidated. Furthermore, questions regarding PCC-mediated membrane protein integration or assembly can only be addressed in the presence of a bilayer.

A routine approach for the visualization of membrane proteins within a membrane environment is therefore highly desirable. Traditional 2D electron crystallography[21] and the more recent single-particle cryo-EM approach called RSC[22] are limited by the difficulty of generating 2D crystals and the rather low resolution, respectively. Here, we report on a new approach for obtaining subnanometer-resolution

[1]Gene Center, Department for Biochemistry, University of Munich, Munich, Germany. [2]Munich Center for Integrated Protein Science (CIPSM), Department of Chemistry and Biochemistry, Munich, Germany. [3]Department of Physics, Beckman Institute, University of Illinois at Urbana–Champaign, Urbana, Illinois, USA. [4]Departamento de Genética Molecular, Instituto de Fisiología Celular, Circuito Exterior S/N, Ciudad Universitaria, Universidad Nacional Autónoma de México, Mexico City, Mexico. [5]Ultrastrukturnetzwerk, Max Planck Institute for Molecular Genetics, Institut für Medizinische Physik und Biophysik, Charite–Universitätsmedizin Berlin, Berlin, Germany. Correspondence should be addressed to R.B. (beckmann@lmb.uni-muenchen.de).

Received 21 September 2010; accepted 3 February 2011; published online 17 April 2011; doi:10.1038/nsmb.2026

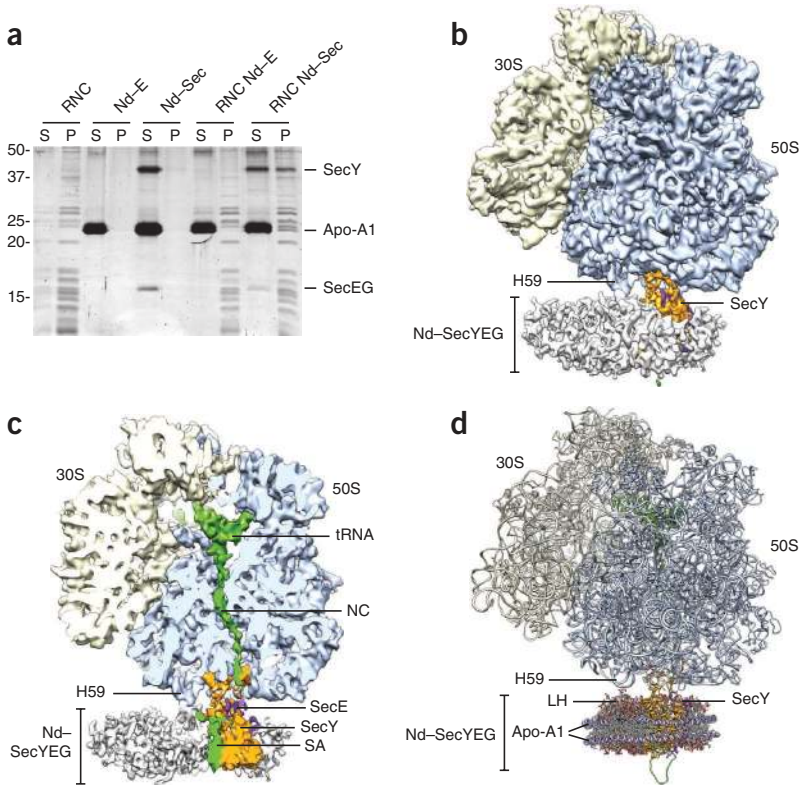

Figure 1 Reconstitution and cryo-EM reconstruction of a 70S RNC–Nd–SecYEG complex. (**a**) Binding assay using purified RNCs (RNC) with an excess of reconstituted Nd–E and Nd–SecYEG (Nd-Sec). Supernatant (S) and pellet (P) fractions were analyzed by SDS-PAGE and SYPRO Orange staining. Nd–SecYEG binds stably to RNCs, whereas Nd–E does not. (**b**) Cryo-EM reconstruction of the active 70S–RNC–Nd–SecYEG complex at 7.1-Å resolution. The ribosomal 30S subunit is shown in yellow, the 50S subunit in blue, SecY in orange, SecE in purple and the Nanodisc in white. (**c**) Density as in **b**, but cut perpendicularly to the plane of the membrane along the polypeptide exit tunnel; colors as in **b** with P-site tRNA, signal anchor (SA) and nascent polypeptide chain (NC) in green. (**d**) All-atom model of the active 70S–RNC–Nd–SecYEG complex. View and colors as in **b**, proteins and RNA in ribbon representation, and phospholipids in ball-and-stick representation with phospholipid head groups (LH) in red-orange, acyl chains in white and apo-A1 in light purple.

structures of membrane protein complexes in a lipid bilayer environment. We integrated the *E. coli* SecYEG complex into high-density lipoprotein (HDL) particles, also termed Nanodiscs, a defined and soluble nanoscale phospholipid bilayer stabilized by a mutant form of apolipoprotein A1 (refs. 23,24), and subjected it, after reconstitution with RNCs, to high-resolution single-particle cryo-EM.

RESULTS

Reconstruction of the ribosome–Nd–SecYEG complex

We purified *E. coli* RNCs[25] carrying an elongation-arrested nascent chain of 118 amino acid residues. The first 102 residues represented the N terminus of the membrane protein FtsQ, preceded by a hemagglutinin (HA) tag and a histidine (His) tag for affinity purification. This type II membrane protein contains an N-terminal signal-anchor transmembrane (TM) helix that was shown to insert co-translationally into the membrane and to remain in contact with SecY and lipids after insertion[26]. Nanodiscs were reconstituted with a mutant form of apolipoprotein A1 (apo-A1 Δ1–43) as described before[23] using *E. coli* total lipid extract in the absence or presence of purified recombinant *E. coli* SecYEG complex. This resulted in Nanodiscs containing only lipids (Nd–E) or containing SecYEG (Nd–SecYEG).

Nascent FtsQ-carrying RNCs were then reconstituted with an excess of Nd–SecYEG and were used in binding assays to test whether the RNC-Nanodisc interaction was dependent on SecYEG. Stable binding of RNCs was observed only in the presence of Nd–SecYEG (**Fig. 1a**), indicating that neither the ribosome nor the signal anchor domain of the nascent FtsQ could interact with, or insert into, the lipid bilayer in a SecYEG-independent manner. We therefore concluded that the reconstituted complexes indeed represented RNC–Nd–SecYEG complexes.

The cryo-EM reconstruction of this complex shows the appearance of a programmed 70S ribosome at 7.1-Å resolution with an additional disc-like density beneath the ribosomal exit site (**Fig. 1b** and **Supplementary Fig. 1**). This density had a diameter of 10–12 nm and a height of about 4–5 nm, tethered by several contacts to the ribosome. The appearance of a clear tRNA density in the P-site confirmed the presence of the nascent FtsQ chain as peptidyl-tRNA. It was possible to visualize the density of the nascent chain within the ribosomal exit tunnel reaching from the peptidyltransferase center (PTC) into the Nd–SecYEG density (**Fig. 1c**). The ribosome contacted the Nd–SecYEG density via several connections, yet leaving a gap on one side of about 15–25 Å between the ribosome and the Nd–SecYEG. This gap is in agreement with data obtained from detergent solubilized complexes[15,16,19], indicating the lack of a seal between the ribosome and the membrane-embedded PCC[27]. The gap suffices to provide the space required for folding or egress of cytosolic domains of membrane proteins.

To interpret the cryo-EM map on a molecular level, we docked crystal structures and molecular models into the density and applied molecular dynamics flexible fitting (MDFF)[28], resulting in a complete molecular model for the 70S–RNC–Nd–SecYEG complex (**Fig. 1d** and **Supplementary Methods**). This model was used as a starting point for a 16-ns molecular dynamics (MD) simulation.

Structure of the Nanodisc

The region of the map representing the Nanodisc was expected to consist of a lipid bilayer with an upper and lower membrane leaflet stabilized by two belt-like apo-A1 Δ1–43 molecules surrounding it. The observed density indeed shows the characteristic dimension of a lipid bilayer with a thickness of about 43 Å (**Fig. 2a**). Strong electron density for the phospholipid head groups was present that could be distinguished from the very weak density for the region occupied by the acyl chains of the fatty acids (**Fig. 2a**). This distribution resembles that observed in membrane-containing viruses[29,30] and in liposomes[31]. In contrast to the phosphate head groups, the acyl chains of the lipids yield very weak electron density because of their composition of low-contrast carbon and hydrogen atoms. The overall dimensions of the electron density representing the Nanodisc are in good agreement with a molecular model for nascent discoidal HDL,

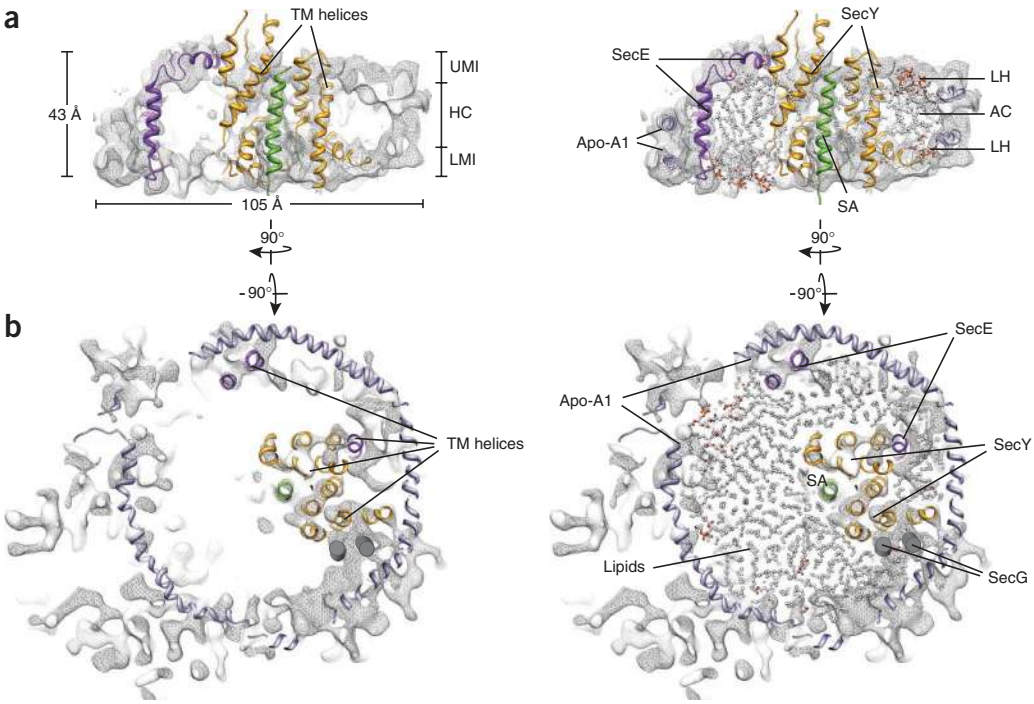

Figure 2 Structure of the Nanodisc. (**a**) Left, side view cut perpendicularly to the plane of the membrane of the isolated electron density of the Nanodisc–SecYEG complex (Nd–SecYEG), showing the lateral gate of SecY. The electron density is represented as a transparent gray mesh with the ribbon representation of the fitted model of a SecY (orange), SecE (purple) and the signal anchor (SA) sequence (green). Two layers of density are visible (upper membrane interface, UMI, and lower membrane interface, LMI), separated by a region of lower density (hydrophobic core, HC) containing transmembrane (TM) helices. Dimensions are indicated. Right, same view, with the fitted Nanodisc model containing lipids in ball-and-stick representation. Phospholipid head groups (LH) are in red (oxygen) and orange (phosphate), acyl chains in white (AC, carbon-hydrogen groups). (**b**) Left, horizontal section, sliced within the plane of the membrane within the hydrophobic core of the lipid bilayer. Rod-like features are visible in the interior of the Nanodisc and account for density of a monomeric SecYEG complex. Right, horizontal section with fitted lipids.

determined using hydrogen-deuterium exchange mass spectrometry or X-ray crystallography of the protein alone[24,32,33]. The outer ring of the Nanodisc, suggested to be composed of two parallel copies of apo-A1 Δ1–43, also shows a stronger density than the lipid acyl chains (**Fig. 2**). However, the density did not allow for the resolution of the protein belts. Nevertheless, we used a current molecular model for apo-A1 (ref. 32) and added lipids to complete our modeling effort for the MD simulation. Fragmented density outside the main disc may be a result of heterogeneity of the disc diameter or of the presence of nonlipidated N-terminal regions of apo-A1 Δ1–43, respectively. Within the bilayer, we found rod-like structures directly beneath the ribosomal tunnel exit, apparently representing the TM helices of the SecYEG complex (**Fig. 2** and **Supplementary Fig. 1c**). The resolution of the Nanodisc appears to be somewhat lower than that of the ribosome. However, the appearance of the rod-like densities representing α-helical regions of SecYE indicates that the resolution for the SecYE complex in the Nanodisc is in the subnanometer range. Our observation shows that the overall dimensions of the membrane protein–containing Nanodisc resemble those of a small circular lipid bilayer, which can be subjected to structure analysis at subnanometer resolution.

Model of the ribosome–SecYE complex and contacts

Based on the previously observed contacts of the cytosolic loops L8/9 and L6/7 of SecY–Sec61 to the ribosome[10,11,13] (**Supplementary Fig. 2**), we fitted a homology model of *E. coli* SecYE into our density by MDFF (**Fig. 3a**). Using the structure of SecYE in the SecYE–SecA complex[4] as a template, we found that the C-terminal half of SecY fitted remarkably well, and only small adjustments of the N-terminal TM helices of SecY were necessary (**Fig. 3a**,**b** and **Supplementary Fig. 3a**,**b**). The position of the short plug helix 2a remained essentially identical to that observed in the SecYE–SecA structure. The N-terminal TM helices of SecE were placed into two additional rod-like densities, guided by the 2D crystal structure of the SecYEG complex[34,35] (**Supplementary Fig. 3c**,**d**). Although we also observed some density in the region where SecG was expected[4] (**Fig. 2b** and **Supplementary Fig. 3d**,**e**), we could not unambiguously identify its exact position, indicating a higher degree of flexibility. Notably, the fitted model left a rod-like density in the proposed lateral gate of SecY unaccounted for, which we interpreted as the inserted signal anchor helix of FtsQ (**Fig. 2** and **Supplementary Fig. 3d**). The MD simulation revealed a stable behavior of the fitted model of the PCC (**Supplementary Fig. 4a**) that, together with a cross-correlation analysis of the quality of the fit, supports its accuracy (**Supplementary Table 1**). Furthermore, the connections between SecYE and the ribosome were maintained throughout the simulation (**Supplementary Fig. 5**), and the position of the signal anchor TM domain was stable with respect to the PCC (**Supplementary Fig. 4b**).

A multitude of contacts were identified between the ribosome and SecYE as well as lipids (**Fig. 3** and **Supplementary Tables 2–6**). The cytoplasmic loops L8/9 and L6/7 of SecY reached into the ribosomal exit tunnel and contacted ribosomal RNA (rRNA) helices H50-H53-H59 and H6-H24-H50, respectively (**Fig. 3a**,**c**,**e**,**f**). Furthermore, both loops also contacted the ribosomal protein L23 in different regions (**Supplementary Tables 2–6**). Notably, the binding mode we observed in the presence of a signal sequence and a lipid bilayer is very similar

to the mode found in inactive complexes and in detergent solution[10,11,13,14]. Thus, this interaction seems to represent the canonical binding mode of the Sec complex to the universal ribosomal adaptor site for both prokaryotic and eukaryotic complexes. An additional contact was likely to represent the C terminus of SecY, contacting ribosomal protein L24 and rRNA helices H24-H50 (**Fig. 3a**,**e**,**f**). A contribution of the SecY C terminus to ribosome binding is in agreement with recent findings for both the bacterial[14] and the eukaryotic system[13] as well as with mutational studies revealing translocation defects of C-terminally truncated SecY[36]. In addition to SecY, SecE also contributes to the interaction of the PCC with the ribosome (**Fig. 3c**,**e**,**f**), consistent with previous data[10,11,13,14]. We observed several contacts between the N terminus as well as the amphipathic helix of SecE and the ribosomal adaptor site proteins L23 and L29, respectively. A stretch of conserved residues in the amphipathic helix of SecE[37] appeared to be involved in contacting both SecY and L23-L29. Although they are in agreement with several previous studies[10–14], these findings are difficult to reconcile with the interpretation by Mitra *et al.*[9]

Notably, the Nd–SecYEG-bound ribosome interacted not only with the PCC but also with lipids. A strong density between rRNA

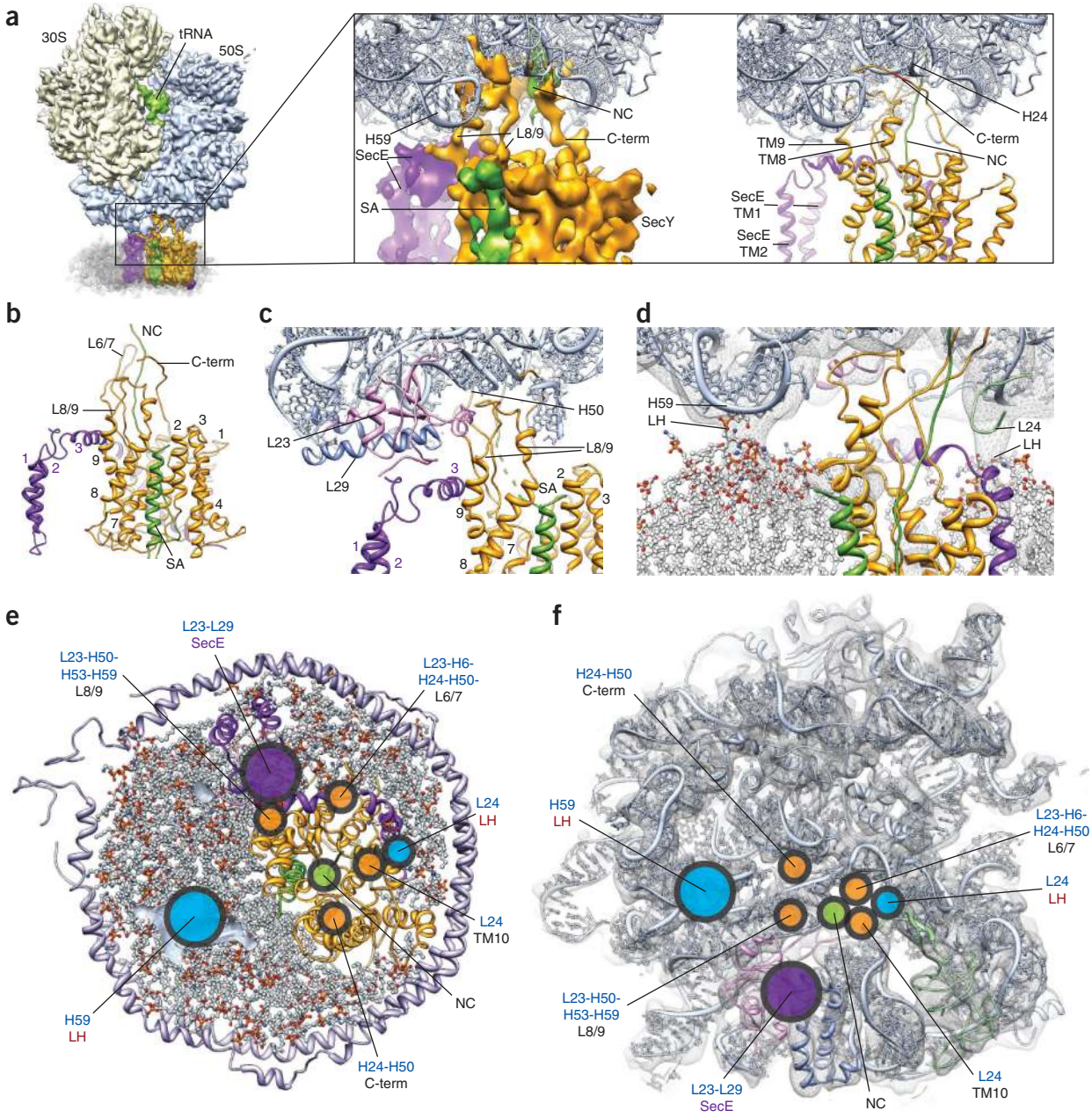

Figure 3 Structure and connections of the membrane-embedded open SecYEG–RNC complex. (**a**) Cryo-EM reconstruction of the 70S–RNC–Nd–SecYEG complex; colors and abbreviations as in **Figure 1**. Insert, molecular model of the 50S subunit with electron density (left) and molecular model for SecYE (right). NC, nascent chain; SA, signal anchor; TM, transmembrane. (**b**) Model of the open SecYE complex with SA (green) residing within the lateral gate, view cut perpendicular to the plane of the membrane. Numbers denote transmembrane domains. (**c**) Close-up of the interaction area of universal ribosomal adaptor site and SecYE. (**d**) Molecular model of the ribosome–SecYE–membrane interface with transparent density filtered at 9–10 Å. Lipid head groups (LH) are indicated. (**e**) Cytoplasmic view of the molecular model of the Nd–SecYE complex with contacts to the 50S subunit indicated by circles. (**f**) View of the ribosomal tunnel exit site; contact sites as in **e**.

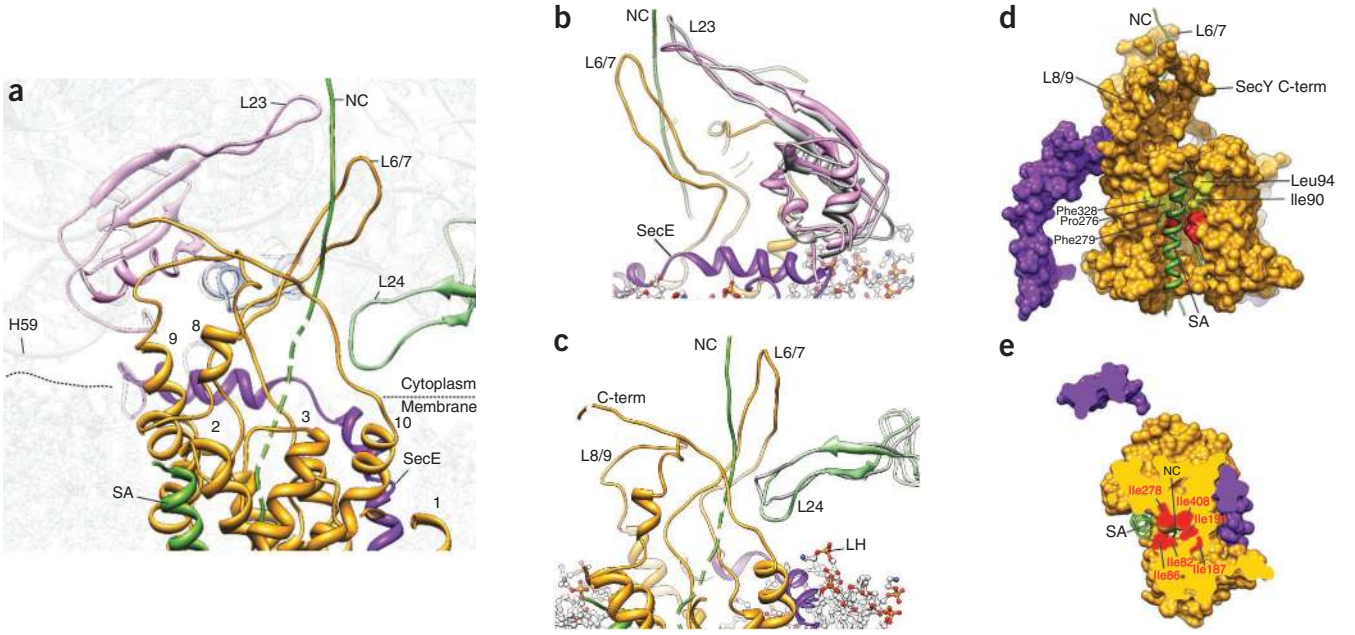

Figure 4 Path of the nascent chain and signal anchor. (**a**) Section through molecular models of the ribosomal exit tunnel and Nd–SecYE. The nascent chain (NC) with the signal anchor (SA) is shown in green. The dotted line indicates the cytoplasm–membrane interface. (**b**) Conformational changes of L23. Comparison of the model of L23 (gray) of an inactive ribosome (PDB: 2i2v) and of L23 (pink) in the presence of a nascent chain (NC; green), SecY (orange), SecE (purple) and lipid head groups. The intra-tunnel loop of L23 bends toward the nascent chain, close to L6/7 of SecY. (**c**) Conformational change of the β-hairpin loop of L24. Comparison of the model of L24 (gray) of an inactive ribosome (PDB: 2i2v) and of L24 (green) in the presence of a nascent chain (green), SecY (orange), SecY C terminus (C-term), SecE (purple) and lipid head groups (LH). (**d**) View of the lateral gate of SecYE shown as a surface representation. SecY is shown in orange, SecE in purple and the nascent chain in green. Conserved residues of SecY that contribute to the central hydrophobic pore ring are indicated in red, and hydrophobic residues of the hydrophobic crevasse that have been found by mutational analysis to be critical for SecY function[5] are indicated in pale yellow. (**e**) View of the position of the SA from the cytoplasmic side, sliced within the plane of the membrane. Hydrophobic pore ring residues are indicated in red.

helix H59 and the disc is apparently mediated by a direct contact to lipid head groups (**Figs. 1b–d** and **3d** and **Supplementary Movie 1**), which is in agreement with previous observations[11,14]. In addition, L24 showed a strong contact with the Nd–SecYEG density that may also involve lipids. After the initial fitting of molecular models, we carried out a molecular dynamics simulation of the ribosome–Nd–SecYE–lipid model with a lipid bilayer that comprises 75% phosphatidylethanolamine and 25% phosphatidylglycerol, mimicking the composition of the bacterial plasma membrane.

Initially, we fitted a flat lipid bilayer into the Nanodisc density; however, shortly after the start, the simulation showed a stable attraction between lipids and rRNA helix H59 (**Supplementary Movie 1**). The resulting lipid distribution resembled the electron density remarkably well, indicating that H59 is indeed capable of establishing another interaction site between the ribosome and the membrane–PCC complex (**Fig. 3d**). In contrast, the additional interactions between L24 and lipids, which were also in good agreement with our electron density, were intermittent, as L24 was seen to interact preferentially with SecY and the nascent chain later in the simulation. The direct interaction of the ribosome with the lipid bilayer, in addition to the SecYE contacts, may explain the rigid positioning of the entire disc with respect to the ribosome and the asymmetrical position of the SecY complex in the disc. Taken together, these data show that a multitude of contacts between ribosome and the C-terminal half of the PCC as well as lipids results in a robust coordination of the ribosome with respect to the membrane surface (**Fig. 3e**,**f**). The observed conformation orients the ribosomal surface around the tunnel exit almost parallel to the surface of the membrane, while leaving a distance of about 20 Å on one side (**Supplementary Fig. 6**). The position of the lateral gate of SecYEG with respect to the ribosomal–PCC contacts would easily facilitate egress of the cytoplasmic domains of nascent peptides alongside the H59 contact away from the main interaction sites.

Model and path of the translocating polypeptide chain

The resolution of the electron density allowed for the tracing of the nascent polypeptide chain from the PTC through the ribosomal exit tunnel (**Fig. 1c**). Furthermore, in the membrane, one rod-like density at the lateral gate of the PCC is best explained by the presence of the inserted signal anchor of FtsQ (**Fig. 4** and **Supplementary Fig. 3b**). After passing the central constriction of the ribosomal tunnel with an unaltered loop region of L22 (**Supplementary Fig. 7a**), the nascent chain engages in a number of contacts in the lower half of the tunnel involving the ribosomal proteins L23, L24 and SecY (**Fig. 4a** and **Supplementary Tables 2–6**). Notably, protein loops participate in all of these contacts and undergo conformational changes as compared to structures of inactive complexes. The conserved loop of L23 that reaches up the tunnel wall has been suggested to constitute a potential interaction site for nascent proteins[38], possibly leading to an inside-to-outside signaling of the nascent chain[39]. In our complex, the tip of L23 (**Fig. 4b**) indeed shifts down as compared to empty ribosomes analyzed by cryo-EM or X-ray crystallography (**Supplementary Fig. 7b**). In the immediate vicinity, the nascent chain subsequently contacts the tip of L6/7 of SecY that embraces the nascent chain. This may indicate a putative role of L6/7 as a sensor for the presence and/or the nature of the nascent chain inside the ribosomal tunnel. Notably, when interacting with an empty ribosome, L6/7 of SecY showed a

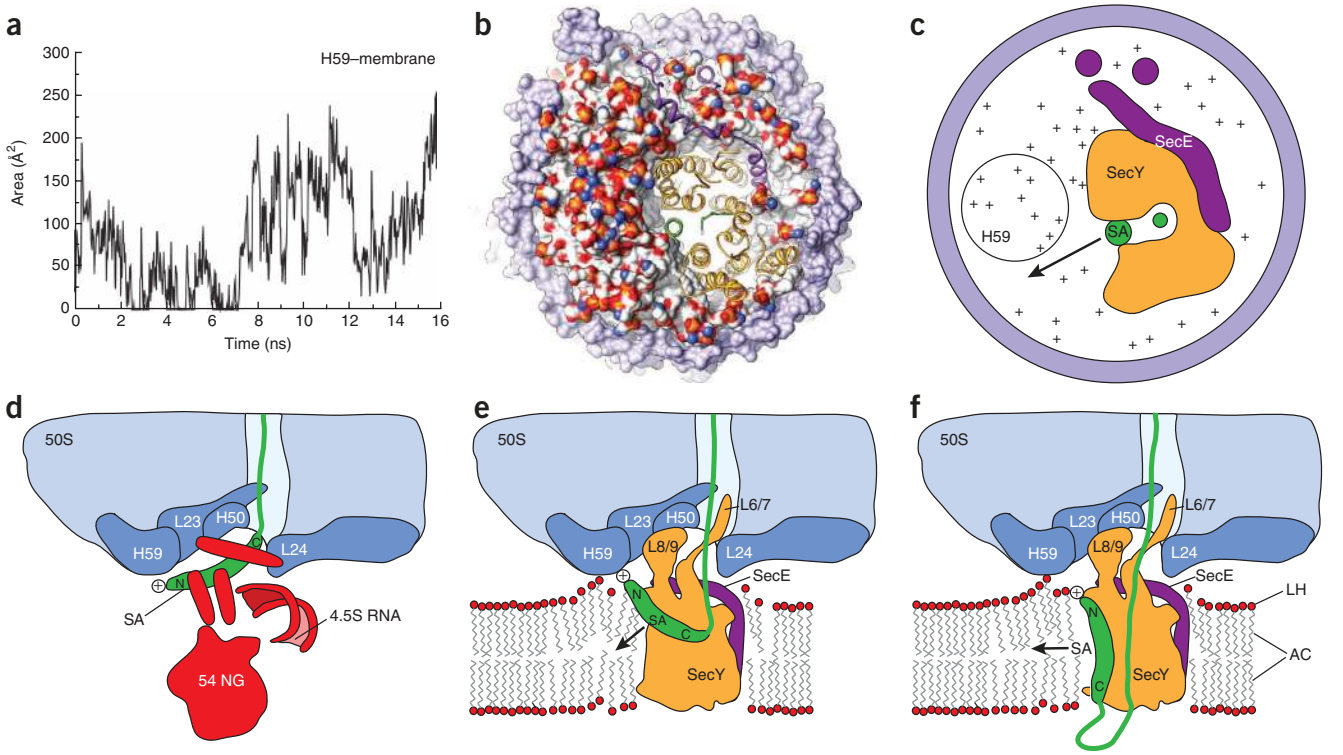

Figure 5 Molecular dynamics simulation and membrane insertion. (**a**) Plot of surface area formed between lipids and ribosomal helix H59 during the MD simulation. (**b**) Surface representation of the Nd–SecYE complex seen from the ribosome after 16 ns MD simulation. Apo-A1 is shown in light purple, SecY in orange, SecE in purple and nascent chain in green, and the atoms of the lipid head groups are colored in orange (phosphate), red (oxygen) and blue (nitrogen), respectively. Note the accumulation of positive charges in the region close to H59 and the disorder of the lipids forming a groove juxtaposed to the signal anchor (SA). (**c**) Schematic depiction of the view in **b** using the same color code and indicating the probable path of the nascent TM domain for integration into the bilayer. (**d**) Schematic depiction of the bacterial 50S ribosomal subunit (blue) bound to the SRP (red; 4.5S RNA and the N-terminal 54 NG domain) in the presence of a signal anchor sequence as observed before[25]. The nascent chain (NC) with the signal anchor (SA) is shown in green. (**e**) Schematic depiction of a hypothetical TM domain insertion intermediate showing the bacterial 50S ribosomal subunit (blue) bound to the SecYEG complex (orange) in the presence of a signal anchor, accessing the hydrophobic lipid phase through a partially open lateral gate. (**f**) Schematic depiction of the observed insertion intermediate with the signal anchor TM domain fully inserted into the lateral gate and exposed to the hydrophobic core of the bilayer. Note the proximity of the SA position as observed in the targeting complex (**d**) and in the insertion intermediate (**e**,**f**). AC, acyl chains; LH, lipid head groups.

different conformation that occluded the tunnel[10] (**Supplementary Fig. 8**). This might be of functional relevance after termination and reinitiation of translation when a newly arriving nascent chain could regulate dissociation of the PCC from the ribosome by interfering with L6/7. When finally exiting the ribosomal tunnel, the nascent chain contacts the exposed β-hairpin of L24 (**Fig. 4c**). This hairpin loop is also bent downward to probably contact the lipid surface and the C terminus of SecY. Taken together, these observations suggest that the nascent chain is carefully guided by protein loops through the ribosomal tunnel to its site of insertion into the PCC.

At the resolution used, we could not trace the path of the complete nascent chain within the PCC. Yet we aimed at building a full model, and we therefore generated a hypothetical path of the nascent chain within the SecY core, based on published biochemical data[8] and in agreement with our SecY model. Therefore, after fitting the TM helices of SecY, we simply extended the nascent chain model from the cytoplasmic to the periplasmic side through the central pore[8], as indicated by a dashed line (**Fig. 4a**). In our SecYE model, the central opening leaves enough space for an extended polypeptide chain to pass, yet a substantial flow of ions would be prevented in the presence of a translocating peptide.

To obtain a complete model for MD simulations, we then connected the nascent chain model (dashed line) with the signal anchor within the proposed lateral gate of the PCC, resulting in the loop-like arrangement expected for a type II membrane protein. Adjusting the SecYE complex from the SecA-activated, pre-open conformation[4] of the template to our map resulted in a laterally open conformation (**Supplementary Fig. 9**). Notably, mainly the gate helices and the N-terminal half of SecY underwent movements, whereas the TMs of the C-terminal half superimposed well with the structure of the pre-open state (**Supplementary Fig. 9a**). This conformation permitted the fitting of the additional signal anchor helix into the rod-like density within the lateral gate (**Fig. 4** and **Supplementary Figs. 1c**, **3b**, **9** and **10**).

The resulting model provides a plausible scenario with an overall arrangement that is in agreement with previous biochemical and structural data. In this model the signal anchor is exposed toward the lipid bilayer, yet it remains tightly enframed by TM2b, TM7 and TM8 of SecY, which may indeed act as the lateral gate for TM domains for insertion into the membrane[3,4,40]. This signal anchor position explains chemical cross-link data that indicate that, at a similar chain length, the signal anchor of FtsQ is in close proximity to both SecY and lipids[26]. Upon further chain elongation, complete release of the signal anchor from SecY is likely to be triggered by additional factors, such as YidC[41,42]. The position of the signal anchor in the lateral gate is also consistent with contacts to conserved hydrophobic residues of SecY TM2, TM7 and TM8 (refs. 5,8) (**Fig. 4d**,**e**) as well as with contacts to residues that can be cross-linked to the signal sequence of

proOmpA[8]. During the MD simulation, the signal anchor remained stable with respect to SecYE (**Supplementary Fig. 4**). Notably, virtually no hydrogen bonds, but mainly hydrophobic interactions, were observed between the signal anchor and SecY (**Supplementary Fig. 10** and **Supplementary Tables 2–6**). Whereas a substantial number of hydrogen bonds would reduce the TM domain's ability to exit into the bilayer, hydrophobic interactions would be in agreement with partitioning according to the TM domain's hydrophobicity. Although we cannot exclude limited flexibility of the signal anchor, the robust density argues in favor of high occupancy in the observed position. Taken together, these data indicate that the signal anchor is in a reasonable and meaningful position in the structure. The positively charged N terminus of the FtsQ signal anchor could remain on the cytosolic side, stabilized by additional interactions with either the phospholipid head groups or the negatively charged phosphate backbone of the nearby rRNA helix H59. At the same time, the position of the signal anchor would prevent phospholipids from entering the center of the PCC. In conclusion, the suggested TM helix at the interface between the lateral gate of SecY and the lipid bilayer as positioned in our model may represent an intermediate step of TM integration into the membrane.

Insertion of a TM domain into the membrane

Both our map and the MD simulation revealed a stable attraction between lipids and rRNA helix H59 (**Figs. 3d** and **5a**, **Supplementary Fig. 11** and **Supplementary Table 7**). Notably, this lipid–H59 interaction resulted in a redistribution of the lipids that affected the immediate vicinity of the suggested TM domain insertion region (**Fig. 5a–c**). The lateral diffusion of lipids is decreased around H59, and the cytoplasmic leaflet of the membrane is less ordered. Similar findings have been reported in a number of recent studies, highlighting the fact that RNA-lipid interactions are based on electrostatic attractions[43–46]. Notably, RNA binding to lipid bilayers may influence and change the bilayer state[45]. In particular, RNAs can even insert into bilayers and perturb membrane permeability[44]. In addition, it has been shown that RNA-lipid binding may lead to lateral segregation and the formation of domains with different compositions in the lipid bilayer[43]. This is in good agreement with our cryo-EM–density and MD-simulation finding that ribosomal rRNA H59 indeed attracts the charged head groups (**Supplementary Table 7**), leading to a disorder in the lipid bilayer in proximity to the lateral gate of SecY. We speculate that this induced disorder may favor membrane insertion of TM domains by decreasing the energy barrier for the TM to access the hydrophobic core of the lipid bilayer through the layer of charged head groups. This is supported by the idea that insertion efficiency is determined by the energetic cost of distorting the bilayer in the vicinity of the TM helix, as predicted by MD simulations[47]. By interacting with positively charged N-terminal residues of TM domains, H59 might even contribute to the correct orientation of TM domains according to the positive-inside rule[48].

When comparing our model to the bacterial RNC–SRP complex[25], we found the positions of the signal anchor domain to be in close proximity to each other (**Fig. 5d** and **Supplementary Fig. 12**). Notably, apart from the previously observed removal of the NG domain of SRP from its L23 binding site[25], only minor conformational adjustments would be required for a concomitant binding of SRP and the SecYEG complex to the ribosome. For transfer from the targeting system to the PCC, the signal anchor could slide from the SRP54 M domain directly into the lateral gate–lipid region of the SecYEG complex (**Fig. 5e** and **Supplementary Fig. 12**). A virtually continuous hydrophobic environment for the insertion of the TM domain into the lipid phase would be provided. The hydrophilic residues that follow the signal anchor would then be oriented in the hydrophilic central conduit of the channel, resulting in the loop-like insertion of the nascent polypeptide (**Fig. 5d–f**).

DISCUSSION

Our subnanometer-resolution cryo-EM structure of the bacterial ribosome–SecYEG complex in a Nanodisc allows for the molecular interpretation of a membrane protein, the SecYEG complex, in its natural lipid bilayer environment. We suggest an insertion intermediate of a type II membrane protein using the proposed lateral gate of the SecYEG complex for partitioning into the lipid phase. Molecular dynamics simulations based on our structure reveal stable interactions between ribosomal RNA and the membrane that may contribute to the insertase activity of the PCC. Using nascent polytopic membrane proteins, future studies will address the mechanism of more complex membrane insertion events. This method may provide a general approach to visualizing functional membrane proteins in the lipid environment by high-resolution single-particle cryo-EM.

METHODS

Methods and any associated references are available in the online version of the paper at http://www.nature.com/nsmb/.

Accession codes. Coordinates of the atomic model and the cryo-EM map have been deposited in the PDB with accession codes 3J00 and 3J01 and in the 3D EM database (EMD–1858), respectively.

Note: Supplementary information is available on the Nature Structural & Molecular Biology website.

ACKNOWLEDGMENTS

We thank B. Seidelt for help with the RNC preparation, J.P. Armache for help with data processing, S. Feuerstein (Forschungszentrum Jülich) for providing the plasmid encoding the apolipoprotein construct, J. Buerger and C. Ungewickell for help with the electron microscopy and D. Wilson for critical discussions. This research was supported by a Boehringer Ingelheim Fonds fellowship (to J.F.), by an Alexander von Humboldt Foundation fellowship and a Human Frontiers Science Program long term fellowship (to E.O.v.d.S.), by a Dr. Klaus Römer Stiftung fellowship (to T.B.), by grants from the Deutsche Forschungsgemeinschaft SFB594 and SFB646 (to R.B.) and SFB 740 (to T.M.), by US National Institutes of Health grants P41-RR005969 and R01-GM067887 (to K.S.), by US National Science Foundation (NSF) grant PHY0822613 (to K.S.) by an Alexander von Humboldt Foundation award (to K.S.) and by the European Union and Senatsverwaltung für Wissenschaft, Forschung und Kultur Berlin (UltraStructureNetwork, Anwenderzentrum). Computer time for MD simulations and MDFF was provided through NSF Large Resources Allocation Committee grant MCA93S028.

AUTHOR CONTRIBUTIONS

J.F. prepared the sample, collected the EM data, performed the 3D reconstruction and built the molecular model; J.G. did the MDFF and the MD simulations. E.O.v.d.S., S.F. and B.B. contributed to the purification of SecYEG; M.G. contributed to the data processing. T.M. and O.B. contributed to the EM data collection. T.B. contributed to model building and interpretation. All authors contributed to the study design and to writing the manuscript.

COMPETING FINANCIAL INTERESTS

The authors declare no competing financial interests.

Published online at http://www.nature.com/nsmb/.
Reprints and permissions information is available online at http://www.nature.com/reprints/index.html.

1. Rapoport, T.A. Protein translocation across the eukaryotic endoplasmic reticulum and bacterial plasma membranes. *Nature* **450**, 663–669 (2007).
2. Halic, M. & Beckmann, R. The signal recognition particle and its interactions during protein targeting. *Curr. Opin. Struct. Biol.* **15**, 116–125 (2005).
3. Van den Berg, B. *et al.* X-ray structure of a protein-conducting channel. *Nature* **427**, 36–44 (2004).
4. Zimmer, J., Nam, Y. & Rapoport, T.A. Structure of a complex of the ATPase SecA and the protein-translocation channel. *Nature* **455**, 936–943 (2008).

5. Tsukazaki, T. *et al.* Conformational transition of Sec machinery inferred from bacterial SecYE structures. *Nature* **455**, 988–991 (2008).
6. Egea, P.F. & Stroud, R.M. Lateral opening of a translocon upon entry of protein suggests the mechanism of insertion into membranes. *Proc. Natl. Acad. Sci. USA* **107**, 17182–17187 (2010).
7. du Plessis, D.J., Berrelkamp, G., Nouwen, N. & Driessen, A.J. The lateral gate of SecYEG opens during protein translocation. *J. Biol. Chem.* **284**, 15805–15814 (2009).
8. Osborne, A.R. & Rapoport, T.A. Protein translocation is mediated by oligomers of the SecY complex with one SecY copy forming the channel. *Cell* **129**, 97–110 (2007).
9. Mitra, K. *et al.* Structure of the *E. coli* protein-conducting channel bound to a translating ribosome. *Nature* **438**, 318–324 (2005).
10. Menetret, J.-F. *et al.* Ribosome binding of a single copy of the SecY complex: implications for protein translocation. *Mol. Cell* **28**, 1083–1092 (2007).
11. Menetret, J.-F. *et al.* Single copies of Sec61 and TRAP associate with a nontranslating mammalian ribosome. *Structure* **16**, 1126–1137 (2008).
12. Kalies, K.U., Stokes, V. & Hartmann, E. A single Sec61 complex functions as a protein-conducting channel. *Biochim. Biophys. Acta* **1783**, 2375–2383 (2008).
13. Becker, T. *et al.* Structure of monomeric yeast and mammalian Sec61 complexes interacting with the translating ribosome. *Science* **326**, 1369–1373 (2009).
14. Gumbart, J., Trabuco, L.G., Schreiner, E., Villa, E. & Schulten, K. Regulation of the protein–conducting channel by a bound ribosome. *Structure* **17**, 1453–1464 (2009).
15. Beckmann, R. *et al.* Architecture of the protein-conducting channel associated with the translating 80S ribosome. *Cell* **107**, 361–372 (2001).
16. Beckmann, R. *et al.* Alignment of conduits for the nascent polypeptide chain in the ribosome-Sec61 complex. *Science* **278**, 2123–2126 (1997).
17. Menetret, J.-F. *et al.* Architecture of the ribosome-channel complex derived from native membranes. *J. Mol. Biol.* **348**, 445–457 (2005).
18. Morgan, D.G., Menetret, J.F., Neuhof, A., Rapoport, T.A. & Akey, C.W. Structure of the mammalian ribosome-channel complex at 17A resolution. *J. Mol. Biol.* **324**, 871–886 (2002).
19. Menetret, J.-F. *et al.* The structure of ribosome-channel complexes engaged in protein translocation. *Mol. Cell* **6**, 1219–1232 (2000).
20. Matlack, K.E., Plath, K., Misselwitz, B. & Rapoport, T.A. Protein transport by purified yeast Sec complex and Kar2p without membranes. *Science* **277**, 938–941 (1997).
21. Raunser, S. & Walz, T. Electron crystallography as a technique to study the structure on membrane proteins in a lipidic environment. *Annu. Rev. Biophys.* **38**, 89–105 (2009).
22. Wang, L. & Sigworth, F.J. Structure of the BK potassium channel in a lipid membrane from electron cryomicroscopy. *Nature* **461**, 292–295 (2009).
23. Alami, M., Dalal, K., Lelj-Garolla, B., Sligar, S.G. & Duong, F. Nanodiscs unravel the interaction between the SecYEG channel and its cytosolic partner SecA. *EMBO J.* **26**, 1995–2004 (2007).
24. Shih, A.Y. *et al.* Molecular modeling of the structural properties and formation of high-density lipoprotein particles. in *Current Topics in Membranes: Computational Modeling of Membrane Bilayers* (ed. Feller, S.) 313–342 (Elsevier, 2008).
25. Halic, M. *et al.* Following the signal sequence from ribosomal tunnel exit to signal recognition particle. *Nature* **444**, 507–511 (2006).
26. Urbanus, M.L. *et al.* Sec-dependent membrane protein insertion: sequential interaction of nascent FtsQ with SecY and YidC. *EMBO Rep.* **2**, 524–529 (2001).
27. Hamman, B.D., Chen, J.C., Johnson, E.E. & Johnson, A.E. The aqueous pore through the translocon has a diameter of 40–60 Å during cotranslational protein translocation at the ER membrane. *Cell* **89**, 535–544 (1997).
28. Trabuco, L.G., Villa, E., Mitra, K., Frank, J. & Schulten, K. Flexible fitting of atomic structures into electron microscopy maps using molecular dynamics. *Structure* **16**, 673–683 (2008).
29. Cockburn, J.J. *et al.* Membrane structure and interactions with protein and DNA in bacteriophage PRD1. *Nature* **432**, 122–125 (2004).
30. Laurinmaki, P.A., Huiskonen, J.T., Bamford, D.H. & Butcher, S.J. Membrane proteins modulate the bilayer curvature in the bacterial virus Bam35. *Structure* **13**, 1819–1828 (2005).
31. Tilley, S.J., Orlova, E.V., Gilbert, R.J., Andrew, P.W. & Saibil, H.R. Structural basis of pore formation by the bacterial toxin pneumolysin. *Cell* **121**, 247–256 (2005).
32. Wu, Z. *et al.* The refined structure of nascent HDL reveals a key functional domain for particle maturation and dysfunction. *Nat. Struct. Mol. Biol.* **14**, 861–868 (2007).
33. Borhani, D.W., Rogers, D.P., Engler, J.A. & Brouillette, C.G. Crystal structure of truncated human apolipoprotein A-I suggests a lipid-bound conformation. *Proc. Natl. Acad. Sci. USA* **94**, 12291–12296 (1997).
34. Breyton, C., Haase, W., Rapoport, T.A., Kuhlbrandt, W. & Collinson, I. Three-dimensional structure of the bacterial protein-translocation complex SecYEG. *Nature* **418**, 662–665 (2002).
35. Collinson, I. The structure of the bacterial protein translocation complex SecYEG. *Biochem. Soc. Trans.* **33**, 1225–1230 (2005).
36. Chiba, K., Mori, H. & Ito, K. Roles of the C-terminal end of SecY in protein translocation and viability of *Escherichia coli*. *J. Bacteriol.* **184**, 2243–2250 (2002).
37. Murphy, C.K. & Beckwith, J. Residues essential for the function of SecE, a membrane component of the *Escherichia coli* secretion apparatus, are located in a conserved cytoplasmic region. *Proc. Natl. Acad. Sci. USA* **91**, 2557–2561 (1994).
38. Houben, E.N., Zarivach, R., Oudega, B. & Luirink, J. Early encounters of a nascent membrane protein: specificity and timing of contacts inside and outside the ribosome. *J. Cell Biol.* **170**, 27–35 (2005).
39. Bornemann, T., Jockel, J., Rodnina, M.V. & Wintermeyer, W. Signal sequence–independent membrane targeting of ribosomes containing short nascent peptides within the exit tunnel. *Nat. Struct. Mol. Biol.* **15**, 494–499 (2008).
40. Gumbart, J. & Schulten, K. Structural determinants of lateral gate opening in the protein translocon. *Biochemistry* **46**, 11147–11157 (2007).
41. Scotti, P.A. *et al.* The *Escherichia coli* homologue of mitochondrial Oxa1p, is a component of the Sec translocase. *EMBO J.* **19**, 542–549 (2000).
42. van der Laan, M., Houben, E.N., Nouwen, N., Luirink, J. & Driessen, A.J. Reconstitution of Sec-dependent membrane protein insertion: nascent FtsQ interacts with YidC in a SecYEG-dependent manner. *EMBO Rep.* **2**, 519–523 (2001).
43. Michanek, A., Kristen, N., Hook, F., Nylander, T. & Sparr, E. RNA and DNA interactions with zwitterionic and charged lipid membranes—a DSC and QCM-D study. *Biochim. Biophys. Acta* **4**, 829–838 (1798).
44. Khvorova, A., Kwak, Y.G., Tamkun, M., Majerfeld, I. & Yarus, M. RNAs that bind and change the permeability of phospholipid membranes. *Proc. Natl. Acad. Sci. USA* **96**, 10649–10654 (1999).
45. Janas, T. & Yarus, M. Specific RNA binding to ordered phospholipid bilayers. *Nucleic Acids Res.* **34**, 2128–2136 (2006).
46. Marty, R., N'Soukpoe-Kossi, C.N., Charbonneau, D.M., Kreplak, L. & Tajmir-Riahi, H.A. Structural characterization of cationic lipid-tRNA complexes. *Nucleic Acids Res.* **37**, 5197–5207 (2009).
47. Jaud, S. *et al.* Insertion of short transmembrane helices by the Sec61 translocon. *Proc. Natl. Acad. Sci. USA* **106**, 11588–11593 (2009).
48. von Heijne, G. The distribution of positively charged residues in bacterial inner membrane proteins correlates with the trans-membrane topology. *EMBO J.* **5**, 3021–3027 (1986).

ONLINE METHODS

Generation of Nanodisc-SecYEG. SecYEG was purified as described previously[49] and then subjected to a gel-filtration step using a Superdex S200 10/30 column and eluted with Sec buffer (10 mM Tris-HCl, pH 8.0, 20% glycerol, 0.05% DDM, 100 mM NaCl). The pooled fractions were concentrated to a final concentration of 2 mg ml^{-1}. Apo-A1 was purified as described before[50]. *E. coli* phospholipids (Avanti Polar Lipids, *E. coli* total extract in chloroform) were dried under a stream of nitrogen and stored in a vacuum exsiccator overnight to remove residual solvent. Lipids were resuspended in cholate buffer (20 mM HEPES, pH 7.2, 100 mM KOAc, 6 mM $Mg(OAc)_2$, 1 mM DTT, 25 mg ml^{-1} cholate) to yield a final concentration of 20 mg ml^{-1} lipids. To reconstitute SecYEG into Nanodiscs, 600 µg apo-A1, 150 µg SecYEG and 300 µg lipids were mixed in a mass ratio of 4:1:2, reconstitution buffer (20 mM HEPES, pH 7.2, 100 mM KOAc, 6 mM $Mg(OAc)_2$, 1 mM DTT, 0.1% DDM) added and the mixture incubated at 37 °C for 1 h. For the preparation of Nanodiscs without SecYEG, the reconstitution mixture contained an equivalent amount of Sec-buffer instead of SecYEG. Subsequently, detergent was removed with Biobeads for 2h at room temperature. The reconstitution mixture was subjected to a gel-filtration step using a Superdex S200 10/30 column and eluted with NDG buffer (20 mM HEPES, pH 7.2, 100 mM KOAc, 6 mM $Mg(OAc)_2$, 1 mM DTT, 10% glycerol). Fractions containing Nanodiscs were pooled and concentrated to 8 pmol $µl^{-1}$.

Purification of *E. coli* 70S RNCs. 70S RNCs carrying a nascent FtsQ polypeptide chain were generated using the *in vitro E. coli* T7 S30 Extract for Circular DNA (Promega) and purified as described before[25] with 16 additional C-terminal amino acids in the FtsQ construct. After the last centrifugation step, the resulting pellet was resuspended slowly in grid buffer (20 mM HEPES, pH 7.2, 50 mM KOAc, 6 mM $Mg(OAc)_2$, 1 mM DTT, 500 µg ml^{-1} chloramphenicol, 0.005% Nikkol (0.5% pill per ml) and 125 mM sucrose), flash frozen and stored at −80 °C.

Reconstitution of *E. coli* 70S RNC–Nd–SecYEG complexes. For binding assays, RNC–Nd–SecYEG complexes were reconstituted by incubating 2 pmol RNCs with 20 pmol Nd–SecYEG for 15 min at 37 °C in a final volume of 25 µl of buffer D (20 mM HEPES-KOH, pH 7.2, 100 mM KOAc, 10 mM $Mg(OAc)_2$, 1 mM DTT, 250 µg ml^{-1} chloramphenicol, 0.5% Complete Protease Inhibitor Cocktail Tablet (Roche) per ml). Binding was tested by centrifugation through a sucrose cushion followed by SDS-PAGE and SYPRO Orange staining.

For electron microscopy, RNC–Nd–SecYEG complexes were reconstituted by incubating 10 pmol RNCs with 80 pmol Nd–SecYEG for 15 min at 37 °C in a final volume of 90 µl of buffer D (20 mM HEPES-KOH, pH 7.2, 100 mM KOAc, 10 mM $Mg(OAc)_2$, 1 mM DTT, 250 µg ml^{-1} chloramphenicol, 0.5% Complete tablet per ml). To remove unbound Nd–SecYEG, the reconstitution mix was spun through a sucrose cushion (20 mM HEPES, pH 7.2, 100 mM KOAc, 10 mM $Mg(OAc)_2$, 750 mM sucrose, 5 mM spermidine, 0.05 mM spermine, 0.5 mM PMSF, 1 mM DTT, 250 µg ml^{-1} chloramphenicol). The resulting pellet was resuspended slowly in grid buffer E (20 mM HEPES, pH 7.2, 100 mM KOAc, 10 mM $Mg(OAc)_2$, 1 mM DTT, 250 µg ml^{-1} chloramphenicol, 0.5% Complete tablet per ml).

Electron microscopy, image processing and modeling. Samples were applied to carbon-coated holey grids according to standard methods[51]. Micrographs were recorded under low-dose conditions on a Tecnai F30 field emission gun electron microscope at 300 kV and scanned on a Heidelberg drum scanner with a pixel size of 1.23 Å on the object scale. The contrast transfer function was determined with CTFFIND and SPIDER[52]. After automated particle picking with Signature[53] followed by visual inspection, a dataset of 520,000 particles was processed with the SPIDER software package and classified into a subset according to Nd–SecYEG presence. 85,664 particles from the *E. coli* RNC–Nd–SecYEG dataset were used for the final contrast transfer function (CTF)-corrected reconstruction with the resolution of 7.1 Å based on the Fourier shell correlation with a cutoff value of 0.5. Models of the *E. coli* 70S structure and tRNA, obtained by X-ray crystallography[54] (PDB: 2I2V) and cryo-EM[55] (PDB: 2WWL, 2WWQ), were fitted into the density and refined by molecular dynamics flexible fitting (MDFF)[28].

Fitting of SecYE and nascent FtsQ. On the basis of the structure of the *Thermotoga maritima* SecYEG[4] (PDB: 3DIN), an *E. coli* SecYE homology model was created using HHpred[56]. Because α-helical secondary structures are resolved within the membrane environment, we obtained a highly reliable rigid body fit by aligning the model according to known ribosomal connections based on the cytosolic loops L8/9 and L6/7 of SecY and on characteristic secondary features of densities representing TM helices 6, 8 and 9. Minor adjustments of the TM helices were carried out using Coot[57]. The N-terminal TM helices of SecE were placed into two additional rod-like densities, the positions of which are in agreement with the 2D crystal structure of the SecYEG[58,59]. These outlying helices have initially been attributed to SecG[59], but in a later paper, after fitting of the *Methanococcus jannaschii* structure into the map, reassigned as the two N-terminal TM helices of SecE[58]. An *ab initio* model of the nascent chain was created using PyMOL (http://www.pymol.org/) and manually fitted into the cryo-EM density using Coot. The combined SecYE-nascent-chain model was refined using MDFF in the presence of the full ribosome, which was constrained during the fitting.

Model and fitting of the Nanodisc. A model of nascent discoidal HDL[32] was used as a template to generate a model for Nd–SecYEG containing 75% phosphatidylethanolamine and 25% phosphatidylglycerol. In our model, we replaced nonstructured elements of the so-called 'solar flares' by a corresponding α-helix with the same amino acid sequence. The Nanodisc model was manually fitted into the density. The lipid bilayer was added to the model with an initially flat profile. Lipids overlapping with SecYE were removed. No MDFF was performed for the Nanodisc proteins or lipid.

Further methods. Further methodology (on MDFF and simulation, including illustrations) are available in the **Supplementary Methods**.

49. van der Does, C., de Keyzer, J., van der Laan, M. & Driessen, A.J. Reconstitution of purified bacterial preprotein translocase in liposomes. *Methods Enzymol.* **372**, 86–98 (2003).
50. Denisov, I.G., Grinkova, Y.V., Lazarides, A.A. & Sligar, S.G. Directed self-assembly of monodisperse phospholipid bilayer Nanodiscs with controlled size. *J. Am. Chem. Soc.* **126**, 3477–3487 (2004).
51. Wagenknecht, T., Grassucci, R. & Frank, J. Electron microscopy and computer image averaging of ice-embedded large ribosomal subunits from Escherichia coli. *J. Mol. Biol.* **199**, 137–147 (1988).
52. Frank, J. *et al.* SPIDER and WEB: processing and visualization of images in 3D electron microscopy and related fields. *J. Struct. Biol.* **116**, 190–199 (1996).
53. Chen, J.Z. & Grigorieff, N. SIGNATURE: a single-particle selection system for molecular electron microscopy. *J. Struct. Biol.* **157**, 168–173 (2007).
54. Berk, V., Zhang, W., Pai, R.D. & Cate, J.H. Structural basis for mRNA and tRNA positioning on the ribosome. *Proc. Natl. Acad. Sci. USA* **103**, 15830–15834 (2006).
55. Seidelt, B. *et al.* Structural insight into nascent polypeptide chain-mediated translational stalling. *Science* **326**, 1412–1415 (2009).
56. Söding, J., Biegert, A. & Lupas, A.N. The HHpred interactive server for protein homology detection and structure prediction. *Nucleic Acids Res.* **33**, W244–8 (2005).
57. Emsley, P. & Cowtan, K. Coot: model-building tools for molecular graphics. *Acta Crystallogr. D Biol. Crystallogr.* **60**, 2126–2132 (2004).
58. Bostina, M., Mohsin, B., Kühlbrandt, W. & Collinson, I. Atomic model of the *E. coli* membrane-bound protein translocation complex SecYEG. *J. Mol. Biol.* **352**, 1035–1043 (2005).
59. Breyton, C., Haase, W., Rapoport, T.A., Kühlbrandt, W. & Collinson, I. Three-dimensional structure of the bacterial protein-translocation complex SecYEG. *Nature* **418**, 662–665 (2002).

doi:10.1038/nsmb.2026